JOINT INSTITUTE FOR NUCLEAR RESEARCH
Dzhelepov Laboratory of Nuclear Problems

FINAL REPORT ON THE INTEREST PROGRAMME

Monte Carlo simulation for shielding evaluation in preclinical SPECT/CT tomography

Supervisor:
Dr. Antonio Leyva Fabelo

Student:
Aliaksandr Miadzvetski, Belarus
Belarusian State University

Participation period:
September 27 – November 05,
Wave 5

Dubna, 2021

Abstract

The use of ionizing radiation sources in medicine can be a threat to the health of personnel. To prevent and minimize the consequences, various methods of protection against ionizing radiation are used. One of the methods of protection is shielding with lead walls. In this work, using GEANT4 and MCNPX code systems based on Monte Carlo methods, the dependence of the dose rate on the distance from the radiation source and the thickness of the lead screen in SPECT and CT was investigated. SPECT technology is based on gamma radiation from radiopharmaceuticals based on ^{201}Tl, ^{99m}Tc, ^{18}F and ^{131}I. CT uses X-ray radiation from an X-ray tube. The results obtained were compared with the maximum safe dose rates recommended by the 103 publication of the ICRP.

Introduction

Application of ionizing radiation in healthcare is basic and routine in contemporary medicine. Benefits to patients from such application have been established beyond doubt [1]. It is difficult to imagine a healthcare system without modern diagnostic imaging and image-guided interventional procedures. A survey of policy leaders in internal medicine rated computed tomography (CT) imaging as one of the main healthcare innovations in the 20th century[2].

However, in order to use these devices, they must meet the conditions. Any device that in this operation uses some source of ionizing radiation, must necessarily guarantee its safety for the health of occupationally exposed personnel. That is why during its development, and before putting it into operation, it requires a large number of tests and trials to ensure that when used they are as harmless as possible to man. For these purposes, mathematical modeling of radiation transfer plays an important role [3, 4].

This work aims to perform the calculation, using the Monte Carlo based code systems Geant4 and MCNPX, of the dose rate distribution with distance for different geometries and sources in a SPECT/CT type preclinical scanner. With these results we intend to determine for each case the distance considered safe for occupationally exposed personnel.

SPECT/CT

a) SPECT

Single photon emission computed tomography (SPECT) is a three-dimensional nuclear medicine imaging technique combining the information gained from scintigraphy with that of computed tomography. This allows the distribution of the radionuclide to be displayed in a three-dimensional manner offering better detail, contrast and spatial information than planar nuclear imaging alone.

SPECT machines combine an array of gamma cameras (ranging from one to four cameras) which rotate around the patient on a gantry. SPECT may be also combined with a separate CT machine in a form of hybrid imaging; single photon emission computed tomography-computerized tomography (SPECT-CT) mainly for the purposes of attenuation correction and anatomical localization [5]. Figure 1 shows the appearance of the scanner.

Figure 1: Siemens single-photon emission computed tomograph.

Detector system rotate around the patient providing spatial information on the distribution of the radionuclide within tissues. The use of multiple detectors increases the efficiency of registration and spatial resolution. The projection data obtained from the detectors are then reconstructed into three-dimensional images usually in axial slices [5-8]. When SPECT-CT is used, attenuation correction and higher resolution anatomical localization can be achieved [5].

b) Computer Tomography

Computed tomography (CT) scanning is a diagnostic imaging procedure that uses x-rays to build cross-sectional images ("slices") of the body. Cross-sections are reconstructed from measurements of attenuation coefficients of x-ray beams in the volume of the object studied [9].

The detectors of the CT scanner measure the transmission of the X-ray beam through a full scan of the body. The image of that section is taken from different angles, and this allows to retrieve the information on the depth (in the third dimension). The appearance of the scanner in Figure 2.

Figure 2: CT scanner.

The CT scanner is made up of three primary systems, including the gantry, the computer, and the operating console. Each of these is composed of various sub-components. The gantry assembly is the largest of these systems. It is made up of all the equipment related to the patient, including the patient support, the positioning couch, the mechanical supports, and the scanner housing. It also contains the heart of the CT scanner, the X-ray tube, as well as detectors that generate and detect X-rays.

Materials and Methods

Sources

A preclinical scanner bases its principles on the same as the clinical scanners discussed here, with the difference that in preclinical ones the dimensions are usually more compact, and the doses are lower. This is because they use as biological targets not humans, but laboratory animals such as mice, rats, rabbits and others. The appearance of such scanner is shown in the Figure 3.

Figure 4: NanoSPECT/CT preclinical scanner

A preclinical SPECT/CT scanner uses two types of radioactive sources. The first is the X-ray tube for the CT, and the second is the gamma radioisotopic source injected into the animal under study for SPECT.

There are four predominant radionuclides used in clinical SPECT imaging: Tc-99m, I-123, F-18 and In-111. The properties of these radionuclides are shown in Table 1.

Table 1: Decay properties of the most common radionuclides used in SPECT and a proposed new clinical radionuclide.

Radioisotope	Half-Life	Energy (intensity)
^{99m}**Tc**	6.02 hours	141 keV (89%)
^{123}**I**	13.22 hours	159 keV (83%)
^{111}**In**	2.80 days	171 keV (91%) and 245 keV (94%)
^{18}**F**	109.7 min	511 keV

The source of X-ray radiation in computed tomography is the X-ray tube shown in Figure 4. For the simulation of the CT configuration, the W anode X-ray tube was approximated to a point source positioned 1 mm in front of the anode. This source emits only in the phantom direction within a solid angle 20^{o}. The full X-ray tube energy spectrum was considered in the simulation and it was calculated using interpolating polynomials (TASMIP) for 120 keV (Figure 5) [10].

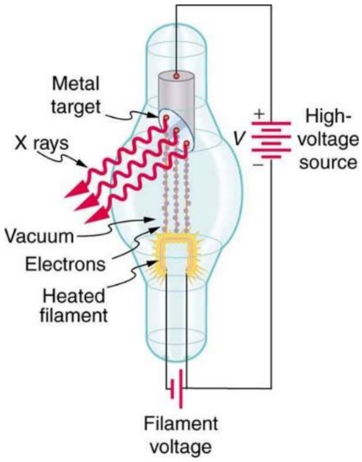

Figure 4: X-ray tube

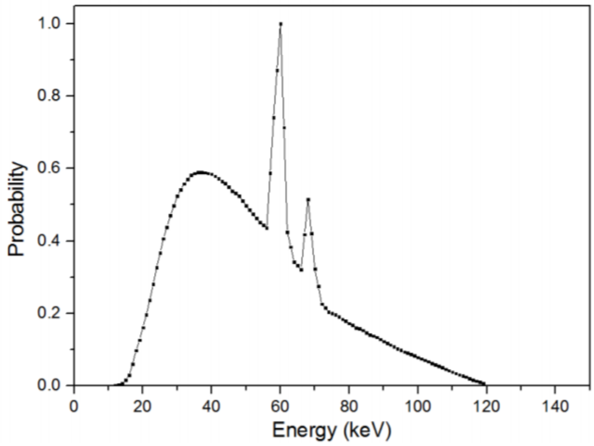

Figure 5. The tungsten anode spectrum

Dose limits

The International Commission on Radiological Protection (ICRP) recommends the safe dose limits [11, 12].
The limits are split into two groups, the public, and occupationally-exposed workers. The dose limit for workers proposed by the ICRP was established as an annual effective dose. As presented in Table 2, an effective dose limit of 20 mSv/year has been set for persons employed in radiation work.

Table 2. Dose limits established for occupationally-exposed workers and public.

	Radiation workers	Public
Effective dose	20 mSv a year, averaged over defined periods of 5 years with no single year >50 mSv	1 mSv a year (higher values are permitted if the average over 5 years is not above 1 mSv a year)
The equivalent dose per year in:		
The lens of the eye	20 mSv a year, averaged over defined periods of 5 years with no single year >50 mSv	15 mSv a year
Skin	500 mSv a year	50 mSv a year
Hands and feet	500 mSv a year	50 mSv a year

Geant4

GEANT4 is a toolkit for simulating the passage of particles through matter. It includes a complete range of functionality including tracking, geometry, physics models and hits. The physics processes offered cover a comprehensive range, including electromagnetic, hadronic and optical processes, a large set of long-lived particles, materials and elements, over a wide energy range starting, in some cases, from 250 eV and extending in others to the TeV energy range. It has been designed and constructed to expose the physics models utilized, to handle complex geometries, and to enable its easy adaptation for optimal use in different sets of applications. The toolkit is the result of a worldwide collaboration of physicists and software engineers. It has been created exploiting software engineering and object-oriented technology and implemented in the C++ programming language. It has been used in applications in particle physics, nuclear physics, accelerator design, space engineering and medical physics [13].

MCNPX

MCNP is a general-purpose, continuous-energy, generalized geometry, time-dependent Monte Carlo radiation transport code designed to track many particles types over broad ranges of energies. It is the next generation in the series of Monte Carlo transport codes that began at Los Alamos National Laboratory. MCNPX (Monte Carlo N-Particle extended) is capable of simulating particle interactions of 34 different types of particles (nucleons and ions) and 2000+ heavy ions at nearly all energies, including those simulated by MCNP. Specific areas of application include, but are not limited to, radiation protection and dosimetry, radiation shielding, radiography, medical physics, nuclear criticality safety, detector design and analysis, nuclear oil well logging, accelerator target design and analysis, fission and fusion reactor design, decontamination and decommissioning. The code treats an arbitrary 3D dimensional configuration of materials in geometric cells bounded by first- and second-degree surfaces and fourth-degree elliptical tori [14].

Results

a) Geant4

A SPECT model has been developed for simulation in Geant4. The model is shown in the Figure 4, with the captions of the model components.

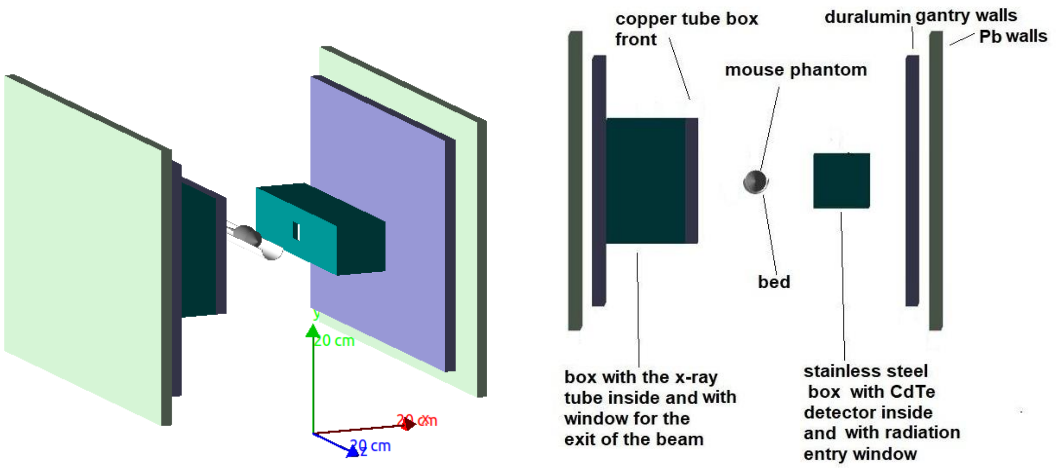

Figure 4: Model of SPECT/CT scanner.

A mouse with a gamma radiation source was placed at the origin (0, 0, 0). Next, the change in the absorbed dose in an elementary cubic volume was studied, for the subsequent conversion to the effective dose. Measurements were carried out at different positions from the radiation source to determine the dependence of the dose rate on distance. The representation of the source inside the target emitting in all direction is shown in Figure 5.

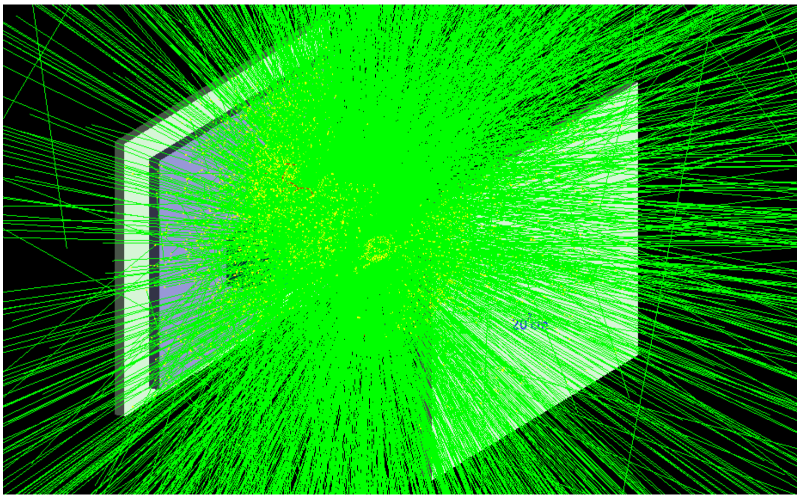

Figure 5: The representation of the source inside the target emitting in all direction in Geant4.

The absorbed dose was determined by the formula:

$$D = \frac{\Delta E_D}{\Delta m} \left[\frac{J}{kg}\right] \tag{1}$$

For the experiment, a source with an activity of 10 MBq was used. As a preliminary result, small dose values of the order of 10^{-12} Gy were obtained at points 5, 10 cm. And at points 15, 20, 25 cm, values of 0 Gy were recorded. Such results are not correct, and it may be related to with an unsuitable detector type for this task. Also, it may be due to an incorrect calculation formula. For example, in [15] and [16], additional coefficients are introduced that consider the features of the material.

There are several ideas for solving this problem. First, try to use a different formula for calculating the absorbed dose. For example, as in [15] and [16]. Second, change the method of obtaining dose, for example, using to search for the flux value at a point using a point detector. It is worth paying attention to the GAMOS library for Geant4, which includes a ready-made implementation of a point detector [17]. To solve the problem by using basic Geant4, it is necessary to implement a point detector yourself. To do this, for example, this manual [18] can be used.

b) MCNPX

A point detector from MCNPX was used to calculate flux (tally F5). The results obtained in units of particles/cm^2 are converted to units of dose, pSv, and then to µSv/h. This conversion is done using the DE, DF and FM cards of the MCNPX.

Figure 6 shows the dependence of the dose rate on the distance for the most commonly used radionuclides. The lines indicate the dose limits of the recommended ICRP [12]. Orange indicates the average maximum dose for occupationally exposed worker and for the lens of the eye, equal to 2.3 µSv/h. Green indicates the maximum dose for the skin, equal to 57.1 µSv/h.

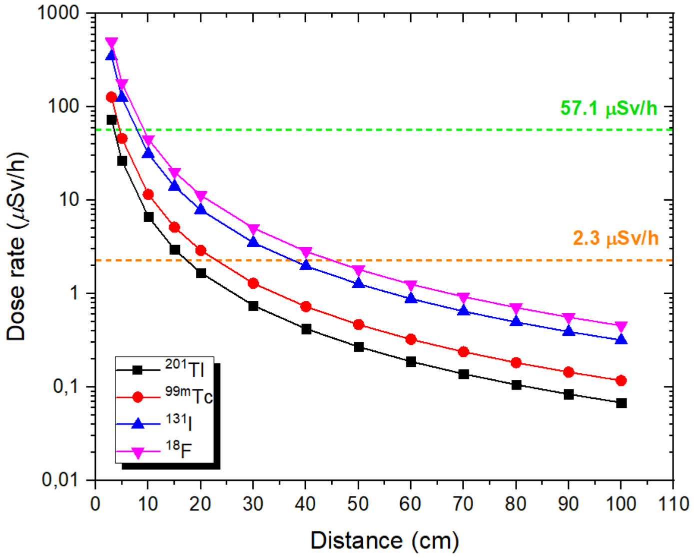

Figure 6: Dose rate vs distance graph for most commonly used radionuclides.

Figures 7-10 show the variations of dose rate as function of distance from the source, for the four gamma sources mentioned above, and for different Pb wall thicknesses (the wall is located 35 cm from the source).

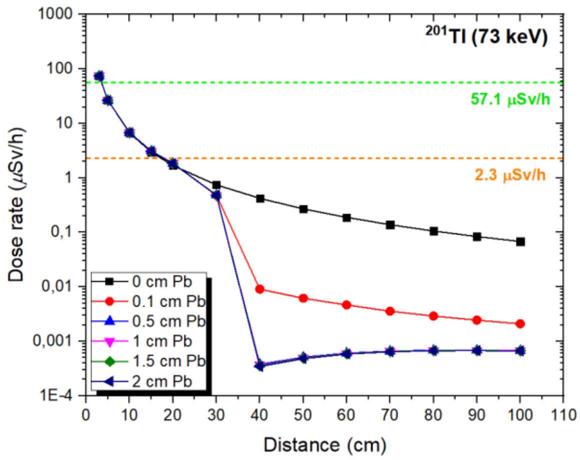

Figure 7: Dose rate vs distance graph for ^{201}Tl.

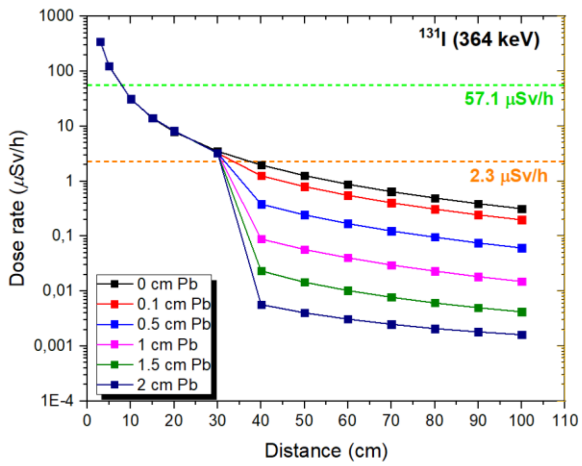

Figure 8: Dose rate vs distance graph for ^{131}I.

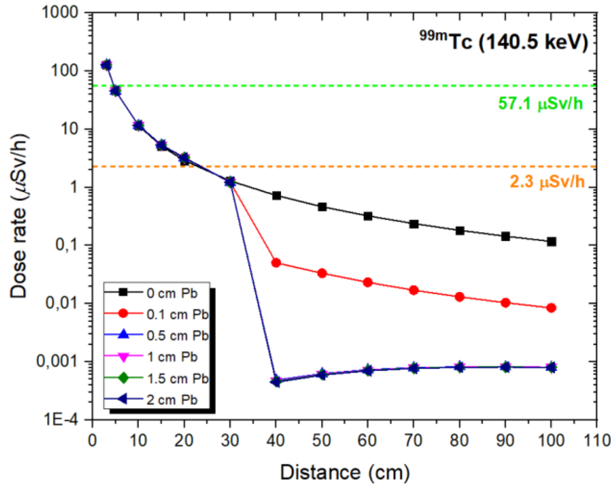

Figure 9: Dose rate vs distance graph for ^{99m}Tc.

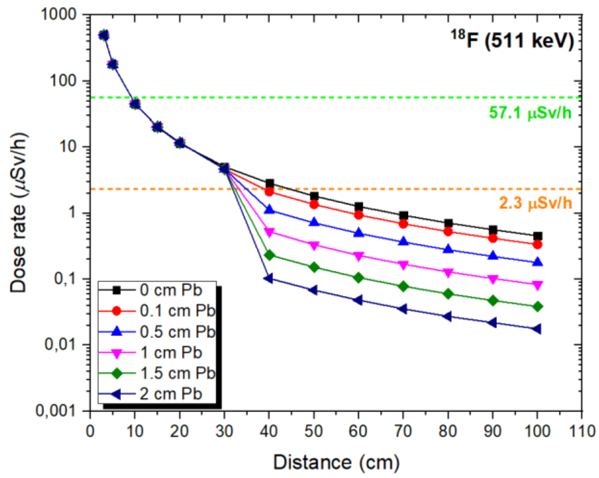

Figure 10: Dose rate vs distance graph for ^{18}F.

From Figures 6-10, we can find the minimum safe distance to meet the recommended standards. The Table 3 shows the values of the minimum distances for 2.3 μSv/h (occupationally exposed worker and cornea of the eyes) and 57.1 μSv/h (skin), depending on and the radiation source.

Table 3. Minimum distance values depending on radionuclides.

Pb wall thickness (cm)	^{18}F		^{99m}Tc		^{131}I		^{201}Tl	
	r_{min} for eyes (cm)	r_{min} for skin (cm)	r_{min} for eyes (cm)	r_{min} for skin (cm)	r_{min} for eyes (cm)	r_{min} for skin (cm)	r_{min} for eyes (cm)	r_{min} for skin (cm)
0	45.3	9.2	23.2	4.41	38.2	7.8	17.6	3.4

From Table 3, it appears that in order to fulfill the recommendations for rationing the effective dose for the skin (57.1 μSv/h), it is unnecessary to apply shielding in the studied configuration. Since gamma radiation is reduced to an acceptable level after passing a distance of 3.4 to 9.2 cm through the bed and air for different radionuclides, even before reaching the protective wall (35 cm).

In order to fulfill the recommendations for rationing the effective dose for occupationally exposed worker and cornea of the eyes (2.3 μSv/h), the minimum safe dose rate level will be obtained at a distance of 17.6 and 23.2, for ^{201}Tl and ^{99m}Tc, respectively (which is less than the distance to the protective wall of 35 cm). It is unnecessary to apply shielding in the studied configuration.

From Figures 6-10, estimating the attenuation produced by the Pb wall at a distance of 40 cm from the source position, the results presented in Table 4 are obtained.

Table 4. Dose rate attenuation produced by Pb wall in % units.

Pb wall thickness (cm)	^{18}F	^{99m}Tc	^{131}I	^{201}Tl
0.1	25.59	93.06	36.54	97.85
0.5	60.94	99.93	80.65	99.91
1	81.54	99.94	95.50	99.91
1.5	91.79	99.94	98.82	99.92
2	96.39	99.94	99.71	99.92

Table 4 shows that the use of a 0.5 cm thick wall for ^{99m}Tc and ^{201}Tl leads to almost complete radiation attenuation (99.9%). For the ^{131}I source, 0.1 cm of Pb wall causes a radiation attenuation of 36.54%, but with 1.0 cm it already reaches 95.5%. For the ^{18}F source, 0.1 cm of Pb wall causes a radiation attenuation of 25.59%, but with 1.5 cm it already reaches 91.79%.

For CT, the simulation was carried out on the same experimental arrangement as for SPECT, except that instead of the point source placed inside the mouse, an X-ray source with W anode was used, positioned in the coordinates (-13.6, 0, 0).

Figure 11 show the variations of dose rate as function of distance from the source (X-rays) for different thicknesses of Pb wall.

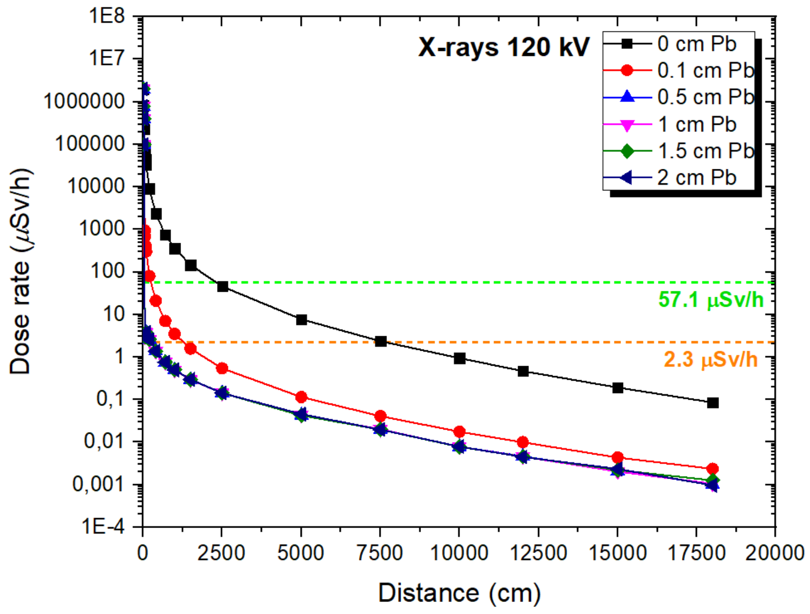

Figure 11: Dose rate vs distance graph for X-rays.

From Figure 11, we can see that the minimum safe distance for the limit in 2.3 μSv/h is 7464.7 cm, and for the limit in 57.1 μSv/h it is equal to 2321 cm.

From Figure 11, estimating the attenuation produced by the Pb wall at a distance of 55 cm from the source position, the results presented in Table 5 are obtained.

Table 5. Dose rate attenuation produced by Pb wall in % units for X-ray.

Pb wall thickness (cm)	Attenuation (%)
0.1	98.958
0.5	99.997
1	99.997
1.5	99.997
2	99.997

The attenuation of radiation observed, at a distance of 55 cm from the source, was 98.96% for 0.1 cm of lead wall; and 99.99% for the rest of the thicknesses studied. These results reveal that there is a maximum thickness value above which increasing this value has no effect on radiation. Table 5 shows how 0.5 cm of thickness is enough to attenuate radiation in a 99.99%.

Taking into consideration that the safe distance values determined here for the CT configuration are relatively large, it is justified, in addition to the protection that the system includes, to use other means of protection for professionally exposed personnel. For example, concrete walls, lead bricks, leaded glass, etc., acting as additional protective barriers, as well as personal protective equipment.

Conclusion

Using the MCNPX and Geant4 code systems for the simulation of radiation transport in materials, the dose rate distribution has been studied in a SPECT/CT scanner prototype. Two typical sources used in these devices were taken into consideration. The first is the sources of gamma radiation, which are the most common isotopes used in medicine (Tc-99m, I-123, F-18 and In-111). The second X-ray radiation from the X-ray tube. The goal was to determine for each, the minimum distance to the source that can be considered safe for occupationally exposed personnel. The minimum permissible distances for the skin and cornea of the eyes were also determined.

The presence of the arrangement of the protective walls made no considerable differences on the minimum safe distance for three sources, remaining 17.6 cm, 23.2 cm and 38.2 cm for ^{201}TI, ^{99m}Tc and ^{131}I, respectively. Hence, for these radioisotopes, it is possible to construct a simple preclinical SPECT device where no protection walls are considered since the safe distance from the source, for an occupationally exposed worker, is small enough to operate and guarantee his safety without the lead wall. However, it is recommended to use shielding to use the ^{18}F isotope. The minimum safe distance when using this isotope without Pb wall protection is equal to 45.3 cm.

The minimum allowable distance for the skin is small and also does not require additional shielding

Calculations of radiation attenuation in the walls were also carried out. In result, for ^{201}TI and ^{99m}Tc, 0.1 cm of the thickness of lead wall attenuates the radiation in a 98 and 93%, respectively; for ^{131}I, 1.0 cm of the thickness of the wall is necessary to reach 95.5% of radiation attenuation; for ^{18}F 1.5 cm of the thickness of the wall is necessary to reach 92% of radiation attenuation

The dose rate vs distance for CT configuration, in absence of any protection wall, showed a minimum safe distance of 7464.7 cm for 2.3 μSv/h and 2321 for 57.1 μSv/h. The inclusion of a lead wall of 0.1 cm attenuates the radiation a 98.96% and 0.5 cm of thickness increases attenuation up to 99.99%. This result revealed that, for the X-rays source studied, there is a maximum thickness value above which increasing this value has no effect on radiation attenuation. This value is 0.5 cm.

From the results, it can be concluded that it is necessary to use 0.5 cm lead protection, but it does not provide the necessary protection against radiation, in particular X-ray radiation, and it becomes necessary to use other methods of protection.

References

1. ICRP, 2007. Radiological Protection in Medicine. ICRP Publication 105. Ann. ICRP 37 (6).
2. Fuchs, V. R., & Sox, H. C., Jr (2001). Physicians' views of the relative importance of thirty medical innovations. Health affairs (Project Hope), 20(5), 30–42.
3. Scuffham, J., Scuffham, J., Sellin, P., Wilson, M., Seller, P., Veale, M., Jacquesd, S., & Cernik, R. (2012). A CdTe detector for hyperspectral SPECT imaging. Journal of Instrumentation, 7(8).
4. Hsieh J. (2015). Computed Tomography: Principles, Design, Artifacts, and Recent Advances, Third Edition, PM259.
5. Bernsen, M. R., Vaissier, P. E., Van Holen, R., Booij, J., Beekman, F. J., & de Jong, M. (2014). The role of preclinical SPECT in oncological and neurological research in combination with either CT or MRI. European journal of nuclear medicine and molecular imaging, 41 Suppl 1(Suppl 1), S36–S49. https://doi.org/10.1007/s00259-013-2685-3
6. Accorsi R. (2008). Brain single-photon emission CT physics principles. AJNR. American journal of neuroradiology, 29(7), 1247–1256.
7. Funada K. (2018). Investigation of Collimator Broad Correction for Dopamine Transporter SPECT Imaging using Monte-Carlo Simulation, Journal of Nuclear Medicine, 59 (supplement 1) 1846;
8. Kulkarni, K., Khorjekar, G., Mete, M., & Van Nostrand, D. (2017). Number of Foci of Functioning Thyroid Tissue Remaining after Thyroidectomy for Differentiated Thyroid Cancer: Institutional Experience. World journal of nuclear medicine, 16(2), 122–125.
9. Buzug T. M. (2011). Computed Tomography, Handbook of Medical Technology, Springer-Verlag, Berlin Heidelberg.
10. Boone, J. M., & Seibert, J. A. (1997). An accurate method for computer-generating tungsten anode x-ray spectra from 30 to 140 kV. Medical physics, 24(11), 1661–1670.
11. ICRP, 2012 ICRP Statement on Tissue Reactions / Early and Late Effects of Radiation in Normal Tissues and Organs – Threshold Doses for Tissue Reactions in a Radiation Protection Context. ICRP Publication 118. Ann. ICRP 41(1/2).
12. ICRP, 2007. The 2007 Recommendations of the International Commission on Radiological Protection. ICRP Publication 103. Ann. ICRP 37 (2-4).
13. https://geant4.web.cern.ch/
14. Hendricks John S., et. al. (2008). LA-UR-08-2216, “MCNPX 2.6.0 Extensions”, Los Alamos National Laboratory.
15. Jemii, E., & Ghedira, L. (2014). Simulation of the dose rate using a GEANT 4 code. 2014 International Conference on Composite Materials & Renewable Energy Applications (ICCMREA).
16. https://www.radiation-dosimetry.org/what-is-absorbed-dose-definition/
17. http://fismed.ciemat.es/GAMOS/
18. https://geant4-forum.web.cern.ch/t/implementing-a-point-detector-estimator/1931

Acknowledgments

I want to thank Dr. Antonio Leyva Fabelo for project management and his great help in its implementation. It was a wonderful opportunity to work on an interesting project and get a unique practical experience.